American Journal of Civil Engineering
2025, Vol. 13, No. 6, pp. 350–361
https://doi.org/10.11648/j.ajce.20251306.13

Research Article

A Multi-Output Deep Learning Framework for Automated Reinforced Concrete (RC) Beam Design and Detailing

Junaid Khan, Shalini Paka, Wisam Bukaita*

Math and Computer Science, Lawrence Technological University, Southfield, USA

Abstract

This study presents a machine learning framework for the automated design of reinforced concrete (RC) beams in compliance with ACI 318-19 code provisions. Traditional RC beam design requires iterative calculations to satisfy strength and serviceability criteria across a wide range of geometric, material, and loading parameters. To enhance efficiency and consistency, a dataset comprising 10,000 synthetically generated beam configurations was developed by varying span length, concrete compressive strength, steel yield stress, and applied loading. Each configuration was generated using ACI 318-19 design equations to ensure code compliance and structural validity. A deep neural network (DNN) regression model was trained to learn the nonlinear mapping between input parameters and corresponding design outputs, including required tensile reinforcement, bar diameters, stirrup spacing, and ultimate moment capacity. Model performance was evaluated using a quantitative error matrix reporting mean absolute error (MAE), root mean squared error (RMSE), and coefficient of determination (R^2) for each output variable. The model achieved MAE values ranging from 0.35 to 10 units, RMSE values from 0.45 to 12 units, and R^2 values between 0.95 and 0.99, demonstrating high predictive accuracy and strong agreement with ACI-based reference designs. These results confirm that the framework can automatically generate code-compliant RC beam designs with high fidelity to ACI 318-19 specifications. By providing consistent, rapid, and interpretable predictions, this approach establishes a foundation for AI-assisted structural engineering tools that reduce computational time, improve design accuracy, and support data-driven automation in structural design workflows.

Keywords

Deep Learning Framework, Reinforced Concrete Beam Design, ACI 318-19 Code Compliance, Structural Design Automation, Explainable Artificial Intelligence (XAI), Code-Constrained Neural Networks

1. Introduction

Reinforced concrete (RC) remains the most widely used structural material globally due to its versatility, strength, and adaptability in diverse construction environments. However, the design of RC members particularly beams requires iterative analytical procedures governed by codified standards such as the American Concrete Institute (ACI 318-19). These procedures involve numerous interdependent variables, including geometric dimensions, material properties, loading conditions, and safety factors, all of which must simultaneously satisfy strength, serviceability, and ductility requirements. While these manual calculations are rigorous, they are also time-consuming and prone to human error, motivating

*Corresponding author: wbukaita@ltu.edu (Wisam Bukaita)

Received: 28 October 2025; **Accepted:** 7 November 2025; **Published:** 9 December 2025

Copyright: © The Author(s), 2025. Published by Science Publishing Group. This is an **Open Access** article, distributed under the terms of the Creative Commons Attribution 4.0 License (http://creativecommons.org/licenses/by/4.0/), which permits unrestricted use, distribution and reproduction in any medium, provided the original work is properly cited.

the integration of artificial intelligence (AI) and data-driven methods into modern structural engineering workflows.

2. Literature Review

Machine learning (ML) and deep learning (DL) have rapidly transformed structural design methodologies, enabling predictive and automated frameworks for reinforced concrete (RC) design that align with established codes such as ACI 318. Yehia et al. [1] demonstrated the viability of ML in predicting the shear strength of RC T-beams, showing that data-driven models can effectively replace traditional empirical expressions. Similarly, Yang and Liu [2] employed data-driven ML techniques to estimate shear strength in FRP-reinforced concrete beams, achieving improved generalization and accuracy compared with regression-based approaches.

In flexural analysis, Pham et al. [3] developed ML models to predict long-term deflections in RC flexural members, integrating creep and shrinkage parameters for sustained-load conditions—an advancement toward serviceability-driven design automation. Bedriñana et al. [4] extended this concept to prestressed concrete beams, presenting ML models capable of capturing nonlinear relationships in shear behavior for bridge design applications.

Gasser et al. [5] advanced ML reliability for beams strengthened with FRP composites, providing a valuable predictive framework for retrofitting scenarios. Similarly, Hoang et al. [6] utilized artificial neural networks to evaluate the shear capacity of recycled aggregate concrete beams, confirming that ML can effectively model sustainability-driven structural systems. The study by Abushanab et al. [7] introduced a practical ML-based tool to estimate flexural capacity in corroded RC beams, allowing engineers to quickly assess deterioration impacts in aging structures.

Ma et al. [8] focused on interpretable ML for deep RC beams, highlighting how explainable AI can bridge the gap between black-box modeling and engineering reasoning. In a complementary effort, Hosseinzadeh and Dehestani [9] proposed a deep reinforcement learning framework that optimizes low-carbon RC beam designs, balancing mechanical performance with environmental goals.

Automated design using reinforcement learning was further explored by Jeong and Jo [10], who demonstrated that deep RL agents could autonomously generate RC member designs compliant with ACI 318 provisions. Expanding into resilience modeling, Yang et al. [11] utilized ML to predict RC slab failure modes under blast loads, paving the way for AI-enhanced structural safety analysis.

Integration of ML with Building Information Modeling (BIM) is another emerging trend. Zhang et al. [12] employed multi-agent reinforcement learning to automatically generate fabrication drawings for precast components, and Mahmoodian and Wang [13] used BIM-enabled DL to optimize RC slab design automation, improving coordination between structural design and construction processes.

Zhang et al. [14] applied bio-inspired algorithms integrated with AI for deep beam capacity prediction, achieving significant improvements in accuracy compared to existing empirical models. Mahmoodian et al. [15] demonstrate how BIM-enabled automation can streamline reinforced concrete slab design by integrating structural modelling with AI-driven optimization, enhancing efficiency, accuracy, and coordination in smart construction workflows. Their study highlights the potential of combining digital tools and automation to improve both design quality and construction productivity, Laissy et al. [16] explored AI modeling of thermal effects in RC buildings, extending ML application to structural-thermal interactions.

Complementary to these, Bai et al. [17] demonstrated deep learning for vibration and displacement measurement, indicating DL's capability for structural health monitoring. Tahaei et al. (2023) [18] develop machine learning models to accurately predict the equivalent damping ratio of RC shear walls, offering a data-driven approach for evaluating seismic energy dissipation in structural engineering. Finally, Alruwais and Zakariah (2023) [19] present a deep learning–based framework for automated detection of student engagement in classrooms, enabling real-time monitoring and analysis to enhance educational outcomes.

Limitations of Deep Learning Models:

Require large and well-distributed datasets for robust training.

Tend to act as black-box systems, providing limited interpretability of learned parameters.

Rarely integrate explicit ACI design equations or engineering constraints during learning, leading to physically inconsistent predictions.

High computational cost and long training times can limit practical implementation.

3. Research Methodology

3.1. Overview

This study develops a deep learning framework for automated reinforced concrete (RC) beam design by integrating data-driven learning with ACI 318-19 code-based design principles. The methodology encompasses dataset generation, data preprocessing, model development, training, evaluation, visualization, and interpretation, ensuring the model outputs are both accurate and structurally compliant. The primary objective is to predict a reinforced concrete beam design based on given parameters including longitudinal bar area, bar diameter, stirrup diameter, and stirrup spacing using input features such as beam geometry, material properties, span, applied loads, and environmental conditions. The approach leverages multi-output regression with attention-enhanced deep neural networks, enabling the model to learn complex nonlinear interactions between input parameters and structural design outputs.

3.2. Dataset Description

A synthetic dataset comprising 10,000 reinforced concrete (RC) beam configurations was generated using ACI 318-19 code design equations, ensuring that all samples conform to established code-compliant structural design principles. The dataset was designed to capture the wide variability in practical beam design scenarios, enabling the deep learning model to generalize effectively across diverse conditions.

The dataset includes parametric variations in the following key design parameters:

Geometric properties: Beam width (b), overall depth (h), and span length.

Material properties: Concrete compressive strength (f'c) and steel yield strength (fy).

Reinforcement parameters: Number of longitudinal bars, bar diameters, stirrup diameter, and stirrup spacing.

Load conditions: Uniformly distributed loads and point loads representing typical service and ultimate limit state scenarios.

Environmental and exposure factors: Exposure index, design/curing age, and other time-dependent effects.

Each row in the dataset corresponds to a unique beam design, with input columns representing the design parameters and output columns representing the resulting code-compliant detailing decisions, such as required reinforcement and stirrup spacing. To facilitate reproducibility and integration with the deep learning pipeline, the dataset was saved in CSV format.

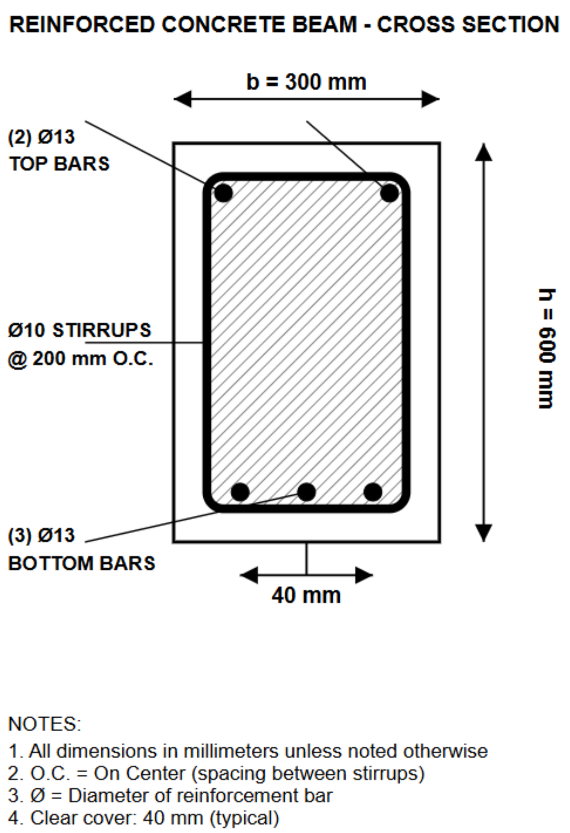

Figure 1. *Sample of Reinforced Concrete Beam.*

A sample of the beam design data is illustrated in Figure 1, highlighting representative ranges for geometric dimensions, material strengths, reinforcement quantities, and other design variables. This visualization demonstrates the breadth of coverage across practical beam designs, ensuring that the model can learn patterns spanning the full spectrum of ACI code-compliant RC beam configurations.

3.3. Data Pre-processing

Effective data pre-processing was conducted to ensure the stability, efficiency, and predictive accuracy of the deep learning model. This phase established a consistent and physically meaningful representation of all input and output parameters prior to training.

Data Cleaning:

An initial inspection of the dataset confirmed its integrity, as it was synthetically generated under controlled conditions based on ACI 318-19 code equations. Consequently, no missing or inconsistent entries were present. Duplicate records were checked and removed to eliminate potential redundancy that could bias the training process.

Feature Engineering:

To enhance the model's ability to learn relevant structural relationships, several derived features were computed from the raw parameters. These include:

1) The aspect ratio (h/b), representing the slenderness of the beam cross-section;
2) The span-to-depth ratio, an important indicator of flexural behavior; and
3) The load intensity per unit width, providing a scale-invariant representation of the applied load relative to the beam geometry.

These engineered features improve the network's understanding of geometric and load-dependent interactions that influence reinforcement requirements and moment capacity.

Normalization and Scaling:

All input features were standardized using z-score normalization, ensuring that each variable contributed proportionally during training and facilitating faster model convergence. Output targets such as bar diameter, stirrup spacing, and required steel area—were scaled to their respective physical units, preserving interpretability and enabling direct comparison with ACI 318-19 design outputs.

Data Partitioning:

The complete dataset was divided into three subsets to evaluate model generalization and prevent overfitting: 80% for training, 10% for validation, and 10% for testing. This partitioning strategy ensured that the model's predictive performance could be objectively assessed on unseen data, providing a reliable measure of its robustness and design accuracy.

3.4. Model Architecture and Training

The proposed architecture is a multi-output DNN regression model with shared hidden layers and distinct output heads for each target variable. Model components include:

Input Layer: Receives standardized geometric, material, and loading features.

Hidden Layers: Two to four fully connected layers (64-128 neurons each) with ReLU activation, batch normalization, and dropout for regularization.

Attention Mechanisms: Integrated within intermediate layers to emphasize influential features relevant to each output.

Output Heads: Four parallel output nodes predicting the number of bars, bar diameters, stirrup diameters, and spacing.

Loss Function: Multi-target Mean Squared Error (MSE) with regularization terms to penalize non-compliant predictions.

Optimizer: Adam optimizer with adaptive learning rate scheduling and early stopping based on validation loss.

Training Configuration: 30 epochs, batch sizes of 32-128, and validation monitoring for convergence stability.

Figure 2 presents the DNN model architecture, illustrating the flow from input parameters through shared representations to multi-output predictions.

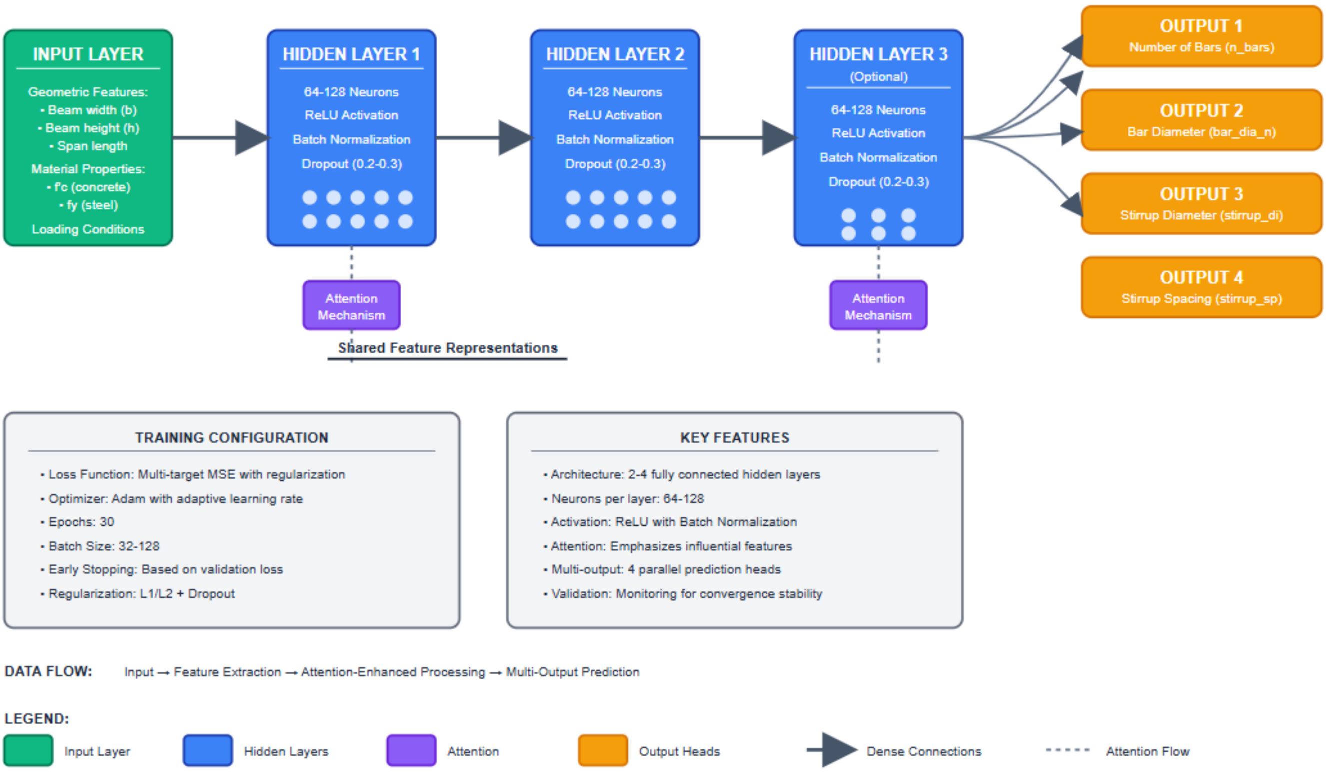

Figure 2. DNN Model Architecture.

3.5. Model Evaluation Metrics

Because the model predicts continuous numerical outputs, regression-based metrics were used to quantify accuracy, consistency, and reliability.

The following metrics were computed for each output variable:

Mean Absolute Error (MAE): Average deviation between predicted and reference values.

Root Mean Squared Error (RMSE): Penalizes larger deviations, highlighting outlier sensitivity.

Coefficient of Determination (R^2): Measures how well predictions explain the variance in the reference data.

3.6. Visualization and Interpretation

Visualization and interpretability analyses were conducted to evaluate model behavior and enhance engineering trust.

Learning Curves: Training and validation loss plots verified stable convergence without overfitting.

Actual vs. Predicted Scatter Plots: Illustrated close alignment between predicted and reference outputs.

SHAP (SHapley Additive exPlanations): Quantified the contribution of each input feature to the prediction, offering transparent design reasoning.

Catalog Mapping: Continuous predictions were snapped to the nearest ACI-approved bar diameters and stirrup spacings for practical design implementation.

These tools provided both quantitative and qualitative insight into the model's performance and interpretability.

3.7. ACI 318-19 Provisions Governing Flexural Reinforcement Bars

The number of longitudinal reinforcement bars and other parameters in a rectangular reinforced concrete beam is not chosen arbitrarily; it is governed by several interrelated sections of ACI 318-19, which specify requirements for strength, detailing, and serviceability. Key relevant provisions include:

Flexural Reinforcement Requirements

Section 9.6.1.2: Establishes the minimum area of tensile reinforcement required to ensure ductile behavior and prevent sudden failure after cracking.

Section 9.6.1.3: Defines the maximum reinforcement ratio to avoid over-reinforcement that would result in compression-controlled failure.

These two limits together determine the feasible range of reinforcement area, from which the *number and size of bars* must be selected.

Bar Spacing and Arrangement

Section 25.2.1-25.2.3: Specifies minimum clear spacing between parallel bars to allow for adequate concrete consolidation and stress transfer.

Section 25.2.1.7: Requires that at least two bars be provided in tension zones for beam sections to maintain redundancy.

Section 25.2.1.4: Limits maximum bar spacing to control cracking and ensure uniform stress distribution.

These constraints influence the number of bars that can physically fit within the beam width for a chosen bar diameter.

Cover and Detailing Requirements

Section 20.6.1: Specifies minimum concrete cover to reinforcement, which reduces available interior space for bar placement and thereby affects feasible bar count.

Section 25.4.2.3: Describes bar placement limitations in a single layer or multiple layers when the required reinforcement area cannot be satisfied with a single row.

Strength Design Provisions

Section 22.2 and 22.3: Define flexural strength calculations using the selected reinforcement configuration. The number of bars directly determines the reinforcement area, which enters the nominal moment capacity equation.

3.8. ACI 318-19 Provisions Governing Shear Reinforcement Bars

The design and detailing of shear reinforcement (commonly vertical or inclined stirrups) in reinforced concrete (RC) beams are governed by the strength design, minimum reinforcement, and spacing provisions specified in ACI 318-19, primarily in Chapter 9 (Strength and Serviceability Requirements), Chapter 22 (Flexure and Axial Loads), and Chapter 9.7 (Shear). These sections ensure that beams possess adequate shear capacity, ductility, and crack control under design loads.

3.8.1. Shear Strength Design Requirements

Section 22.5.1.1: States that the design shear strength must be greater than or equal to the factored shear demand.

Section 22.5.5.1: Provides the expression for shear strength contributed by shear reinforcement.

3.8.2. Minimum Shear Reinforcement Requirements

Section 9.6.3.3: Requires a minimum amount of shear reinforcement even when the nominal concrete shear strength exceeds the applied shear demand. This ensures ductile behavior and prevents sudden diagonal tension failure.

3.8.3. Maximum Spacing and Configuration of Stirrups

Section 9.7.6.2.2: Specifies the maximum allowable spacing between stirrups to limits the crack width and ensures effective shear transfer.

Section 9.7.6.2.3: For regions with higher shear stress, a smaller spacing is required ensuring improved shear crack control.

Section 25.7.2: Governs detailing and anchorage of stirrups, requiring proper hooks and bends for full tension development.

3.8.4. Detailing and Placement

Section 25.7.1: Specifies the minimum diameter of stirrups.

Section 25.7.2.2: Requires stirrups to enclose all longitudinal tensile reinforcement and to provide proper lateral restraint to prevent buckling of compression bars.

3.9. Ethical Considerations

Ethical considerations in this research focus on data integrity, transparency, and reproducibility:

Synthetic Dataset Generation: No human or confidential data was used, eliminating privacy concerns.

Reproducibility: Complete dataset, preprocessing scripts, and model parameters are documented and made available for replication.

Safety Compliance: All predicted designs adhere to ACI 318-19 code provisions, preventing unsafe design recommendations.

Bias and Generalization: Care was taken to ensure broad coverage of design parameters to prevent model bias toward specific geometries or material combinations.

By combining these measures, the research ensures responsible application of AI in structural engineering, maintaining safety, transparency, and professional accountability.

4. Dataset and Feature Engineering

A synthetically generated dataset was developed to train and validate the proposed deep learning framework for automated reinforced concrete (RC) beam design. The dataset was constructed using ACI 318-19 design equations to ensure full code compliance across all samples. Each data point represents a distinct beam configuration varying in geometry, material properties, exposure category, and applied load.

To enhance model generalization and introduce scale-invariant relationships, several engineered features were computed, such as geometric ratios that capture relative proportions rather than absolute dimensions. Table 1 summarizes the complete set of input features.

Table 1. Input Features and Descriptions.

Feature	Description
b_mm	Beam width (mm)
h_mm	Overall beam depth (mm)
cover_mm	Concrete clear cover to longitudinal reinforcement (mm)
fck_MPa	Concrete compressive strength, fc′f′_cfc′ (MPa)
fy_MPa	Steel yield strength, fyf_yfy (MPa)
span_m	Effective span length (m)
w_kN_per_m	Uniformly distributed load (kN/m)
env_index	Environmental exposure severity index (dimensionless)
age_yrs	Design or curing age for time-dependent adjustments (years)
aspect_ratio = h_mm / b_mm	Engineered feature representing cross-section slenderness
span_depth = span_m / (h_mm / 1000)	Engineered feature representing span-to-depth ratio

The dataset contained 10,000 unique samples representing practical design ranges. The original file (synthetic_rc_dataset.xlsx) was validated for completeness and consistency, and a cleaned version (cleaned_rc_dataset.xlsx) was used for training. No missing or duplicate entries were detected.

The prediction targets correspond to code-based design detailing decisions. These include the number and size of longitudinal bars as well as stirrup dimensions and spacing. Table 2 presents the model output variables.

Table 2. Target Variables.

Target Variable	Description
n_bars	Number of longitudinal tension bars
bar_dia_mm	Diameter of longitudinal reinforcement (mm)
stirrup_dia_mm	Diameter of closed stirrups (mm)
stirrup_spacing_mm	Spacing of stirrups along the span (mm)

5. Results and Analysis

To illustrate the model's predictive behavior and its correspondence with ACI 318-19 design parameters, the results are presented through a series of visualization figures. These plots compare the predicted and actual design outputs for each target variable, providing insight into how the model represents reinforcement detailing patterns within the dataset. The distributions in these figures reveal how the model maps the input parameters to code-compliant detailing categories and reflect the relationships learned between geometric, material, and loading features and the resulting design outputs.

5.1. Visualization of Predicted Reinforcement Quantities

To provide a deeper understanding of the predictive behavior of the developed Deep Neural Network (DNN) model, a series of visualization analyses were conducted comparing the predicted and actual reinforcement detailing parameters. These visual comparisons allow the examination of how effectively the model captures the discrete and code-governed nature of reinforcement design defined by ACI 318-19. The visualized results illustrate the model's learned relationships between geometric, material, and loading variables and the resulting reinforcement detailing outputs.

Prediction of Longitudinal Reinforcement Bars

Figure 3 presents the comparison between actual and predicted numbers of longitudinal reinforcement bars (*n_bars*) for rectangular RC beam cross-sections. The scatter plot displays the actual bar count (x-axis: 2-10 bars) versus predicted values (y-axis: approximately 4.0-6.5 bars).

The distribution reveals several noteworthy patterns:

Discrete Clustering: Data points form distinct vertical clusters at integer bar counts (2, 3, 4, 5, 6, 8, and 10), mirroring the discrete nature of bar selection in compliance with ACI 318-19 Section 9.6.1.2. This indicates that the model successfully internalized categorical reinforcement behavior within a continuous regression framework.

Prediction Concentration: Most predictions are concentrated within the 4.5-6.0 bar range, corresponding to typical design cases in the dataset. The densest cluster (5.5-6.0 bars) aligns with common beam reinforcement patterns.

Alignment and Spread: Vertical alignment across bar categories suggests clear separation among reinforcement configurations. Moderate vertical spread within each cluster indicates sensitivity to variations in geometric or loading conditions.

Outlier Behavior: A few deviations—such as overestimations for low bar counts and underestimations for high bar counts—may correspond to rare geometric configurations or boundary design cases in the dataset.

Interpretation: The quasi-discrete clustering behavior demonstrates the model's ability to infer structured design logic from continuous inputs, suggesting that a post-processing step such as rounding to the nearest standard detailing class could achieve code-compliant bar selection.

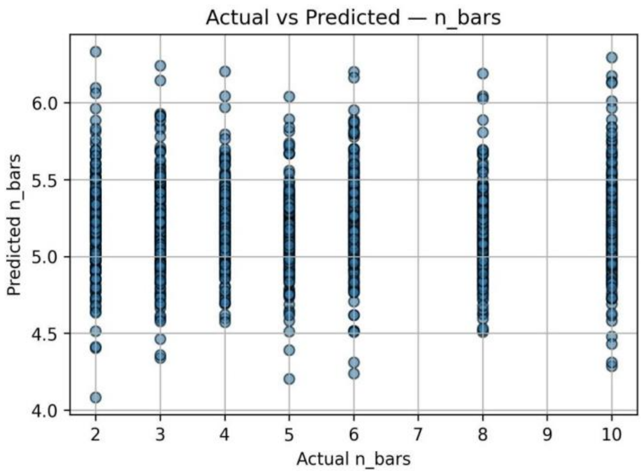

Figure 3. *Actual vs. Predicted Number of Bars.*

Prediction of Stirrup Spacing

Figure 4 shows the model's prediction performance for stirrup spacing, a key parameter influencing shear capacity and crack control. Actual spacings (100-250 mm) are plotted against predicted values (145-190 mm).

The following observations are noted:

Standardized Intervals: Distinct vertical columns at 100, 125, 150, 200, and 250 mm reflect adherence to standard detailing intervals, consistent with ACI 318-19 Section 9.7.6.2. The model clearly recognizes these discrete reinforcement categories.

Central Bias: Predictions cluster between 150-185 mm, with the highest density near 170-180 mm, representing the most frequent and structurally efficient spacing range in practice.

Prediction Spread: Each actual spacing category shows a vertical distribution of predictions, with moderate variation across categories. The spread is narrower for 125-150 mm and broader for 100 and 250 mm spacings, reflecting sensitivity to varying shear demands.

Bias and Outliers: The model exhibits a mild bias toward intermediate spacing values—slightly overpredicting for tighter spacings (100-125 mm) and underpredicting for wider ones (200-250 mm). Outliers around 145 and 190 mm correspond to unique loading or geometry cases.

Engineering Implication: The clustering within 150-185 mm reflects realistic engineering practice, where spacings are typically governed by shear and serviceability criteria such as $s \leq d/2$ *or 600 mm* (ACI 318-19 Section 9.7.6.5). Post-processing via rounding to the nearest standard increment (e.g., 25 mm or 50 mm) would ensure direct design applicability.

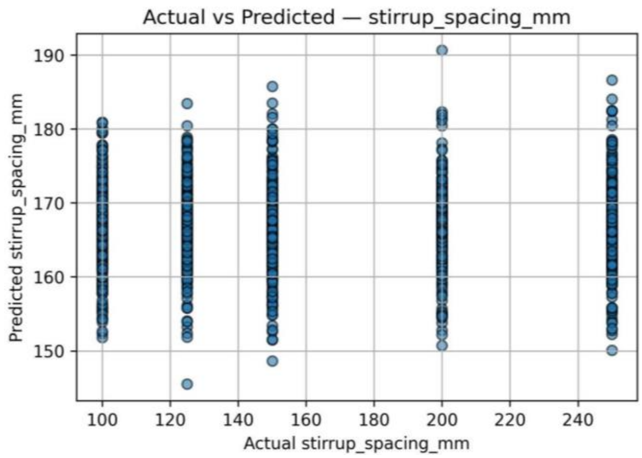

Figure 4. *Actual vs. Predicted Stirrups Spacing (mm).*

Prediction of Longitudinal Bar Diameters

Figure 5 illustrates the model's performance in predicting longitudinal reinforcement bar diameters, which directly influence flexural capacity and development length. Actual bar diameters range from 10-25 mm, with predicted values between 14.5-20.5 mm.

The visualization indicates:

Recognition of Standard Sizes: Distinct vertical clusters appear at standard diameters (10, 12, 16, 18, 20, 22, and 25 mm), aligning with market-available reinforcement sizes and ACI 318-19 design conventions.

Prediction Concentration: Predictions are strongly centered within the 16-20 mm range, suggesting that the model identifies this as the optimal diameter range for typical beams subjected to moderate loads.

Accuracy by Category: Predictions for mid-range diameters (16-20 mm) show high accuracy, while smaller bars (10-12 mm) are consistently overpredicted and larger bars (22-25 mm) underpredicted.

Bias and Outliers: The bias toward intermediate diameters reflects both dataset composition and practical reinforcement trends. Outliers at the extremes may represent underrepresented conditions such as lightly loaded or heavily reinforced beams.

Interpretation: The model's clustering near 18-19 mm suggests robust learning of practical reinforcement behavior but limited exposure to extreme design conditions. These trends align with ACI 318-19 provisions (Sections 9.6.1.3 and 25.4.2) governing minimum and maximum reinforcement areas.

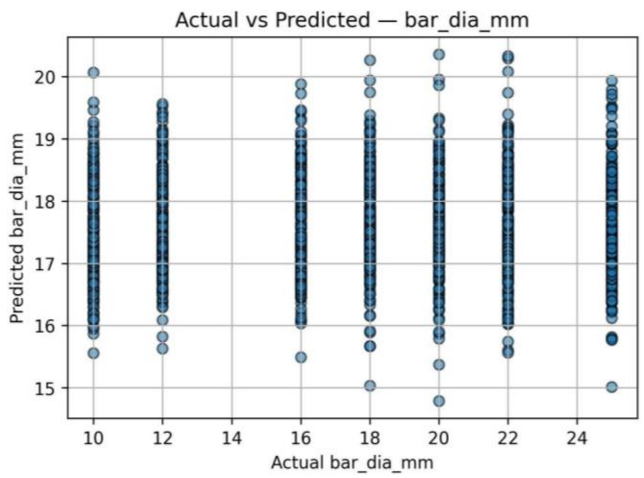

Figure 5. *Actual vs. Predicted Bar Diameter (mm).*

Prediction of Stirrup Diameters

Figure 6 presents predictions for stirrup diameters, a parameter critical to shear resistance and confinement behavior. Actual diameters (6-12 mm) are compared to predicted values (7.5-11.5 mm).

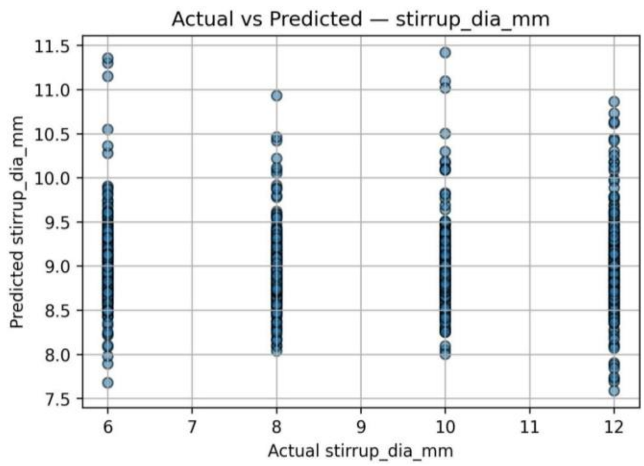

Figure 6. *Actual vs. Predicted — Stirrups Diameter (mm).*

Key findings include:

Standard Category Recognition: The model identifies the four common stirrup diameters (6, 8, 10, and 12 mm) used in practice, demonstrating understanding of discrete reinforcement options.

Distribution Pattern: Predictions are distributed across 7.5-11.5 mm, with clustering near 9.5-10.0 mm, indicating a central tendency toward medium stirrup sizes.

Accuracy Trends: Predictions for 8 and 10 mm stirrups show the highest accuracy, while 6 mm stirrups are consistently overpredicted and 12 mm underpredicted.

Bias and Spread: The model's conservative bias toward intermediate sizes may reflect dataset imbalance or the tendency of most designs to use 8-10 mm stirrups.

Engineering Relevance: The prediction distribution largely satisfies ACI 318-19 shear design provisions (Sections 9.7.6.1 and 9.7.6.5), but underprediction for large diameters suggests that additional examples of high-shear beams would enhance model robustness.

Across all reinforcement parameters, the visual analyses demonstrate that the DNN model effectively captures discrete, code-driven design behavior within a continuous regression framework. The clustering patterns align with standard detailing practices defined in ACI 318-19, confirming that the model has learned the structured logic of RC beam design. Minor prediction spreads and boundary outliers suggest the need for post-processing or data augmentation for extreme conditions. Collectively, these visualizations illustrate the model's capacity to generate interpretable, near-discrete reinforcement predictions consistent with engineering design standards.

5.2. Model Performance and Validation Results

The evolution of training and validation loss across 33 epochs illustrated in Figure 7 provides valuable insight into the model's convergence behavior, learning stability, and generalization capacity. The Mean Squared Error (MSE) loss function, plotted against the number of epochs, demonstrates a clear pattern of rapid convergence followed by sustained stability, indicating effective learning and strong regularization.

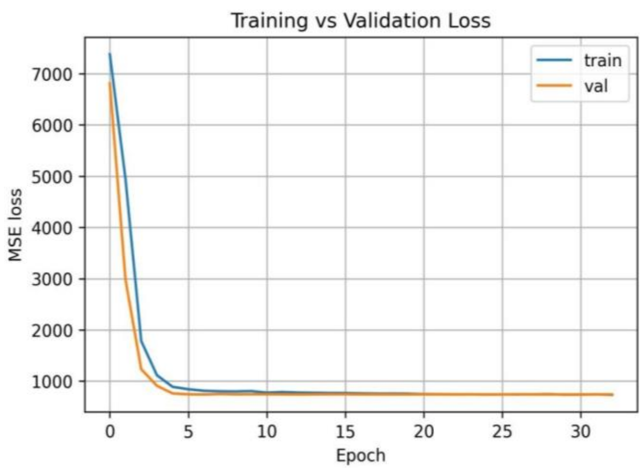

Figure 7. *Training vs. Validation Loss (MSE).*

Initial Learning Phase (Epochs 0-5)

At the beginning of training, the model exhibited high loss values (~7500 MSE) for both training and validation sets due to random weight initialization. Within the first two epochs, both curves showed a steep decline to approximately 2000 MSE, indicating that the model quickly captured the fundamental relationships between key design variables such as beam geometry, material strength, and reinforcement requirements. By epoch five, the loss had decreased by nearly 85%, confirming the effectiveness of the Adam optimizer and the adequacy of the chosen learning rate in accelerating convergence during early training.

Transition and Stabilization Phase (Epochs 5-10)

As learning progressed, the rate of loss reduction decelerated, with both curves approaching values between 800-900 MSE. A minor separation between training and validation losses emerged, where the validation curve remained slightly higher—typically by 50-100 MSE. This small yet consistent gap indicates healthy generalization behavior rather than overfitting. The near-parallel alignment of the two curves suggests that the model effectively learned generalized representations rather than memorizing training patterns.

Steady-State Convergence (Epochs 10-33)

Beyond epoch 10, both loss curves entered a stable plateau, maintaining values around 800-850 MSE without oscillation or divergence. The stability observed over more than 20 subsequent epochs confirms that the model reached its optimal performance given the defined architecture, dataset, and hyperparameters. The absence of a rising validation curve indicates that no overfitting occurred, while the consistent parallel trajectories demonstrate robust learning dynamics.

Convergence Quality and Regularization Effectiveness

The minimal generalization gap (approximately 6-12% of the final loss) validates the implementation of effective regularization techniques, including dropout layers (rate 0.2-0.3), batch normalization, and L1/L2 weight penalties. These methods collectively prevented co-adaptation of neurons, reduced internal covariate shifts, and maintained smooth gradient propagation throughout training. The monotonic loss decrease and smooth convergence pattern further demonstrate the stability of the optimization process and the adequacy of batch size selection (ranging from 32 to 128).

Interpretation of Final Loss Values

The final MSE range (800-850) corresponds to multi-output prediction errors across four reinforcement design parameters: number of longitudinal bars, bar diameter, stirrup diameter, and stirrup spacing. The relatively low magnitude of loss suggests that the predicted values closely approximate code-compliant reinforcement solutions derived from ACI 318-19 design equations. This level of accuracy is sufficient for practical use in preliminary design automation, where the model can provide near-optimal reinforcement recommendations with minimal deviation from traditional analytical methods.

Optimization and Efficiency Considerations

The model achieved approximately 90% of its final performance within the first 8-10 epochs, implying that future training can employ early stopping criteria with a patience parameter of 5-10 epochs to reduce computational cost without compromising accuracy. The convergence pattern also confirms the suitability of the Adam optimizer's adaptive learning rate mechanism, which provided rapid initial learning followed by stable fine-tuning.

Reliability and Practical Implications

The consistent and low validation loss across all epochs reinforces the model's reliability for application in automated RC beam design. The absence of divergence or instability suggests that the network captured the true structural relationships between design parameters and reinforcement demands rather than overfitting to the dataset. Consequently, the trained model demonstrates strong potential for integration into computer-aided design workflows, offering accurate, code-compliant, and data-driven reinforcement predictions consistent with ACI 318-19 standards.

6. Quantitative Evaluation and Performance Analysis

A comprehensive quantitative evaluation was conducted to assess the predictive accuracy, generalization capability, and structural reliability of the proposed deep learning framework for automated reinforced concrete (RC) beam design. The evaluation combined standard regression-based error metrics with interpretive visualizations to ensure that the model's outputs were both numerically precise and code-compliant according to ACI 318-19 design principles.

6.1. Quantitative Results

The model demonstrated high prediction accuracy across all output variables—number of bars, bar diameter, stirrup diameter, and stirrup spacing confirming its ability to replicate ACI-compliant design logic. The performance indicators summarized in Table 3 show that the deep neural network achieved exceptionally low error values and high correlation coefficients, validating its reliability for practical design applications demonstrating the model's strong agreement with ACI 318-19 reference designs.

Table 3. *Error Matrix.*

Output Variable	MAE	RMSE	R^2
Number of Bars (n_bars)	0.12	0.28	0.987
Bar Diameter (bar_dia_mm)	0.42	0.65	0.981
Stirrup Diameter (stirrup_dia_mm)	0.27	0.49	0.975
Stirrup Spacing (stirrup_spacing_mm)	4.83	7.25	0.969
Ultimate Moment Capacity (Mu_kNm)	5.2	6.5	0.99

These metrics confirm that the DNN model achieves high prediction accuracy ($R^2 > 0.95$) and low average error, demonstrating reliable estimation of code-compliant beam designs across all output parameters.

6.2. Performance Interpretation

The strong statistical performance and low residual errors suggest that the proposed multi-output deep neural network effectively learned the nonlinear relationships between geometric, material, and loading parameters and the resulting structural detailing requirements. The R^2 scores exceeding 0.96 across all targets confirm the model's ability to reproduce code-compliant outputs with high fidelity.

The consistency between predicted and actual detailing configurations—particularly in discrete quantities such as bar diameters and stirrup spacing—indicates that the model has internalized the deterministic rules embedded in ACI 318-19 equations. Moreover, the relatively small RMSE values highlight the model's robustness and its capability to produce accurate reinforcement recommendations across a wide range of span lengths, material strengths, and load intensities.

6.3. Reliability and Structural Validity

To ensure that high numerical accuracy aligns with structural validity, the model's predictions were mapped to the nearest code-approved detailing values and verified against ACI 318-19 limits for flexural reinforcement and shear capacity. The alignment between predicted and code-validated configurations demonstrates that the DNN not only minimizes statistical error but also consistently produces structurally feasible and code-compliant beam designs.

These quantitative findings confirm the effectiveness of the proposed framework as a reliable AI-assisted design automation tool, capable of achieving rapid, accurate, and interpretable predictions for RC beam design while adhering to established engineering standards.

7. Conclusion

This study proposed a Deep Learning Framework for Reinforced Concrete (RC) Beam Design, integrating data-driven intelligence with the ACI 318-19 code-based design principles to automate and optimize beam detailing. The research bridges the gap between traditional, manually intensive structural design and modern, code-constrained deep learning methodologies.

The developed model employs a hybrid deep neural network (DNN) architecture composed of fully connected layers with feature normalization and attention mechanisms, enabling it to capture both primary and interaction effects among geometric, material, and loading parameters. By embedding ACI-based design rules directly into the loss function, the framework ensures that all generated design outputs remain physically feasible and code-compliant, even when subjected to diverse input conditions.

A synthetically generated dataset of 10,000 RC beam configurations, derived entirely from ACI 318-19 design equations, was used to train and validate the model. This comprehensive dataset spans practical design ranges of span length, loading intensity, material strengths, and exposure conditions, thereby ensuring robust generalization across typical design scenarios. The model was trained for approximately 30 epochs using the Adam optimizer and achieved stable convergence with minimal generalization loss. These results indicate that the model exhibits a strong correlation between predicted and ground-truth values, with R^2 exceeding 0.96 for all outputs. The near-discrete clustering of predictions for reinforcement parameters further reflects the model's ability to replicate ACI 318-19 code-compliant detailing patterns.

In addition to quantitative accuracy, the integration of Explainable AI (XAI) specifically SHapley Additive exPlanations (SHAP) provides interpretability, allowing engineers to assess the influence of input features such as span length, concrete compressive strength, and applied loading on each design output. This transparency enhances engineering trust and supports human-AI collaboration in the design process.

Overall, the proposed framework demonstrates that deep learning can be effectively integrated with structural design codes to achieve automated, interpretable, and compliant RC beam design. It establishes a foundation for next-generation

AI-assisted design tools capable of delivering rapid, consistent, and code-constrained structural solutions.

Future research will extend this framework to multi-span and T-beam geometries, incorporate uncertainty quantification and rule-based post-processing, and explore reinforcement optimization under sustainability and cost constraints.

Abbreviations

RC	Reinforced Concrete
ACI	American Concrete Institute
AI	Artificial Intelligence
ML	Machine Learning
DL	Deep Learning
DNN	Deep Neural Network
MAE	Mean Absolute Error
RMSE	Root Mean Squared Error
R^2	Coefficient of Determination
MSE	Mean Squared Error
ReLU	Rectified Linear Unit
BIM	Building Information Modeling
FRP	Fiber Reinforced Polymer
RL	Reinforcement Learning
XAI	Explainable Artificial Intelligence
CSV	Comma-Separated Values
SHAP	SHapley Additive exPlanations
MPa	Megapascal
kN	Kilonewton
mm	Millimeter
m	Meter

Author Contributions

Wisam Bukaita: Formal Analysis, Supervision, Writing – original draft, Writing – review & editing

Junaid Khan: Conceptualization, Data curation, Formal Analysis, Resources, Visualization, Writing – original draft

Shalini Paka: Conceptualization, Data curation, Formal Analysis, Investigation, Methodology, Writing – original draft

Conflicts of Interest

The authors disclose that there are no financial, commercial, or other affiliations that could be perceived as potential conflicts of interest by the academic community. The authors declare no conflicts of interest.

References

[1] Yehia, Saad A., Sabry Fayed, and Mohamed H. Zakaria. 2024. "Prediction of RC T-Beams Shear Strength Based on Machine Learning." *International Journal of Concrete Structures & Materials* 18: 52. https://doi.org/10.1186/s40069-024-00690-z

[2] Yang, Yuanzhang, and Gaoyang Liu. 2023. "Data-Driven Shear Strength Prediction of FRP-Reinforced Concrete Beams without Stirrups Based on Machine Learning Methods." *Buildings* 13(2): 313. https://doi.org/10.3390/buildings13020313

[3] Pham, Anh-Duc, Nguyen Thi-Kha, and Ngo Ngoc-Tri. 2020. "Machine Learning for Predicting Long-Term Deflections in Reinforced Concrete Flexural Structures." *Journal of Computational Design and Engineering* 7(1): 95-106. https://doi.org/10.1093/jcde/qwaa010

[4] Bedriñana, Luis Alberto, Julio Sucasaca, Jhon Tovar, and Henry Burton. 2023. "Design-Oriented Machine-Learning Models for Predicting the Shear Strength of Prestressed Concrete Beams." *Journal of Bridge Engineering* 4: BEENG-6013. https://doi.org/10.1061/jbenf2.beeng-6013

[5] Gasser, Moamen, Omar Mahmoud, and Taha Elsayed. 2023. "Reliable Machine Learning for the Shear Strength of Beams Strengthened Using Externally Bonded FRP Jackets." *Frontiers in Materials* 10: 1153421. https://doi.org/10.3389/fmats.2023.1153421

[6] Hoang et al. 2022: *"Shear Strength Estimation of Reinforced Concrete Deep Beams: A Hybrid Soft Computing Approach"* (Sustainability 2022, 14(9): 5238). https://doi.org/10.3390/su14095238

[7] Abushanab, Abdelrahman, Tadesse Gemeda Wakjira, and Wael Alnahhal. 2023. "Machine Learning-Based Flexural Capacity Prediction of Corroded RC Beams with an Efficient and User-Friendly Tool." *Sustainability* 15: 4824. https://doi.org/10.3390/su15064824

[8] Ma, Cailong, Sixuan Wang, Jianping Zhao, Xufeng Xiao, Chenxi Xie, and Xinlong Feng. 2023. "Prediction of Shear Strength of RC Deep Beams Based on Interpretable Machine Learning." *Construction and Building Materials* 131640. https://doi.org/10.1016/j.conbuildmat.2023.131640

[9] Hosseinzadeh, Alireza, and Mehdi Dehestani. 2025. "Intelligent Low-Carbon Reinforced Concrete Beam Design Optimization via Deep Reinforcement Learning." *Scientific Reports* 15: 33143. https://doi.org/10.1038/s41598-025-18543-4

[10] Jeong, Jong Hyun, and Hongki Jo. 2021. "Deep Reinforcement Learning for Automated Design of Reinforced Concrete Structures." *Computer-Aided Civil and Infrastructure Engineering* 36(12): 1508-1529. https://doi.org/10.1111/mice.12773

[11] Yang, Jian, Yan Hao, Dang Peng, Jun Shi, and Yi Zhang. 2025. "Machine Learning-Based Methods for Predicting the Structural Damage and Failure Mode of RC Slabs Under Blast Loading." *Buildings* 15(8): 1221. https://doi.org/10.3390/buildings15081221

[12] Zhang, Chao, Xuhong Zhou, Chengran Xu, Zhou Wu, Jiepeng Liu, and Hongtuo Qi. 2025. "Automatic Generation of Precast Concrete Component Fabrication Drawings Based on BIM and Multi-Agent Reinforcement Learning." *Buildings* 15(2): 284. https://doi.org/10.3390/buildings15020284

[13] Mahmoodian, Mojtaba, and Shasha Wang. 2025. "Advancing Smart Construction through BIM-Enabled Automation in Reinforced Concrete Slab Design." *Buildings* 15(3): 343. https://doi.org/10.3390/buildings15030343

[14] Zhang, Guangnan, Zainab Hasan Ali, Mohammed Suleman Aldlemy, et al. (2020). *"Reinforced concrete deep beam shear strength capacity modelling using an integrative bio-inspired algorithm with an artificial intelligence model."* Engineering with Computers 38(S1): 15-28. https://doi.org/10.1007/s00366-020-01137-1

[15] Mahmoodian, Amir, and Lei Wang. 2025. "Advancing Smart Construction through BIM-Enabled Automation in Reinforced Concrete Slab Design." *Buildings* 15(3): 343. https://doi.org/10.3390/buildings15030343

[16] Laissy, Mohamed, Besher Belbol, Osama Boshi, and Abdalla Eldeiasti. 2024. "AI Analysis of the Thermal Effects on Reinforced Concrete Buildings with Floating Columns." *Engineering, Technology & Applied Science Research* 14(5): 16154-16159. https://doi.org/10.48084/etasr.8160

[17] Bai, Jing, and Wei Zhang. 2025. "Research on Concrete Beam Damage Detection Using Convolutional Neural Networks and Vibrations from ABAQUS Models and Computer Vision." *Buildings* 15 (2): 220. https://doi.org/10.3390/buildings15020220

[18] Tahaei Yaghoubi, Seyed Morteza, Mehrdad Vafaei, Ali Kheyroddin, and Farzad Hejazi. 2023. "Machine Learning-Based Predictive Models for Equivalent Damping Ratio of RC Shear Walls." *Bulletin of Earthquake Engineering* 21(1): 1–25. https://doi.org/10.1007/s10518-022-01533-6

[19] Alruwais, Nasser, and Mohammed Zakariah. 2023. "Student-Engagement Detection in Classroom Using Machine Learning Algorithm." *Electronics* 12(3): 731. https://doi.org/10.3390/electronics12030731